Biosensors and Bioelectronics 24 (2009) 1067–1073

Contents lists available at ScienceDirect

Biosensors and Bioelectronics

journal homepage: www.elsevier.com/locate/bios

Review

Optimizing the cationic conjugated polymer-sensitized fluorescent signal of dye labeled oligonucleotide for biosensor applications

Kan-Yi Pu, Bin Liu*

Department of Chemical and Biomolecular Engineering, 4 Engineering Drive 4, National University of Singapore, Singapore 117576, Singapore

ARTICLE INFO

Article history:
Received 15 April 2008
Received in revised form 8 July 2008
Accepted 9 July 2008
Available online 26 July 2008

Keywords:
Biosensor
Cationic conjugated polymer
Fluorescence resonance energy transfer
Signal amplification

ABSTRACT

Methods for real time, highly selective and sensitive polynucleotide detection are of vast scientific and economic importance. Fluorescence resonance energy transfer (FRET)-based assays which take advantage of the collective response of water-soluble conjugated polymers (CPs) and the self-assembly characteristic of aqueous polyelectrolytes have been widely used for the detection of DNA, RNA, protein and small molecules. The detection sensitivity of CP-based biosensor is dependent on the signal amplification of dye emission upon excitation of CP relative to that upon direct excitation of the dye. Using cationic polyfluorene derivatives and chromophore (fluorescein or Texas Red) labeled single-stranded DNA molecules (ssDNA-C*) as donor/acceptor pairs, we show that in addition to the spectral overlap, orientation and distance between the donor and the acceptor, the energy levels and fluorescence quenching of the donor/acceptor within the polymer/DNA-C* complexes are also important factors that affect the signal output of dye emission.

Contents

1. Introduction

Methods for DNA detection are under intense investigations due to their vital applications, which include clinical diagnosis, environmental monitoring, forensic analysis and antiterrorism (Wang, 2000). Effective DNA-sensing requires selectivity, to identify single-nucleotide polymorphism (SNP), and sensitivity, to provide information from the small quantities of naturally occurring DNAs. Many DNA detection assays have been developed using different principles (Cardullo et al., 1988; Dubertret et al., 2001), such as fluorescence (Sutherland and Mulley, 1989; Chan and Nie, 1998; Bruchez et al., 1998), electrochemical (Boon et al., 2000; Fan et al., 2003), microgravimetric (Mannelli et al., 2003), enzymatic (Patolsky et al., 2001), electroluminescence (Avouris and

* Corresponding author. Tel.: +65 6516 8049; fax: +65 6779 1936.
E-mail address: cheliub@nus.edu.sg (B. Liu).

0956-5663/$ – see front matter © 2008 Elsevier B.V. All rights reserved.
doi:10.1016/j.bios.2008.07.029

Chen, 2006), and recently nanostructure based methods (Nam et al., 2003; Seferos et al., 2007). In general, the detection is constrained or limited by the levels of targets available in a particular sample. One has to rely on enzymatic sample replication (polymerase chain reaction) to increase the concentration of specific nucleic sequences to detectable levels or turn to complex labeling steps (dye multiplicity) or enhanced optical (or instrumentation) systems (Nuovo, 2000). Such remedies are often reagent and instrumentation intensive, inciting high levels of complexity and cost.

Conjugated polymers (CPs) form the basis of new platforms for the trace detection of analytes in a variety of environments (Swager, 1998; Leclerc, 1999; Chen et al., 1999; McQuade et al., 2000; Nilsson and Inganäs, 2003; Liu et al., 2003a; Kim et al., 2004; Pinto and Schanze, 2004; Herland and Inganäs, 2007). Their delocalized electronic structure allows for electronic coupling between optoelectronic segments and efficient intrachain and interchain energy transfer (Nguyen et al., 2000; Thomas et al., 2007). Important properties, such as charge transport (Korri et al., 1997), conductivity (Bäuerle and Emge, 1998), emission intensity (Chen et al., 1999), and exciton migration (Lee and Swager, 2004) are easily perturbed by external agents, leading to substantial changes in measurable signals (Swager, 1998). CP-based sensors are sensitive to minor perturbations, due to amplification by the collective response, and therefore offer advantages when compared with small molecule counterparts (Zhou and Swager, 1995). Introduction of ionic functional groups into conjugated polymers leads to conjugated polyelectrolytes (CPEs), which combine the optoelectronic properties of conjugated polymers with the charge-mediated behaviors of polyelectrolytes (Pinto and Schanze, 2002). Electrochemical and optical DNA sensors based on conjugated polymers (CPs, such as poly(pyrrole), poly(thiophene), poly(phenylenevinylene), etc.) have been reported (Chen et al., 1999; McQuade et al., 2000; Ewbank et al., 2001; Ho and Leclerc, 2004).

A reliable method for DNA detection based on fluorescence resonance energy transfer (FRET) from a cationic-conjugated polymer (CCP) to a signaling chromophore recently emerged (Gaylord et al., 2002, 2003; Liu and Bazan, 2004a). The assay comprises two ingredients: (a) a light harvesting CCP and (b) a probe oligonucleotide attached by a luminescent signaling chromophore (C*). Emission of light characteristic of the signaling C*, upon excitation of the CCP, indicates the presence of the target oligonucleotide. Transduction by electrostatic interactions induced energy transfer is an essential component of the general strategy. In one approach, a fluorescein (Fl) tagged peptide nucleic acid (PNA) sequence was used as the probe (Gaylord et al., 2002). Hybridization of the neutral PNA-Fl to the complementary single-stranded DNA (ssDNA) results in duplex formation and the incorporation of Fl onto a macromolecule with net negative charges. Electrostatic attraction between the duplex and CCP brings the dye sufficiently close to the CCP to favor FRET. In the presence of a non-complementary DNA, hybridization does not occur and the CP binds preferentially to ssDNA. One determines whether the target strand is complementary to the PNA probe by monitoring the Fl emission upon CCP excitation. When chromophore-labeled ssDNA (ssDNA-C*) is used as the singling probe instead of PNA-Fl, Coulombic screening by the non-complementary ssDNA is insufficient, which results in some Fl emission in the presence of a non-complementary sequence (Gaylord et al., 2003). However, the ssDNA-C* and CCP system, due to its simplicity, has been widely utilized to investigate of the factors that affect FRET (Bazan, 2007; Liu and Bazan, 2004a, 2006b).

The detection sensitivity of CCP-based biosensor is dependent on the signal amplification of C* emission upon excitation of CCP relative to that upon direct excitation of C* (Liu and Bazan, 2004a, 2005). *Amplification factor* is defined as the intensity ratio of the saturated CCP-sensitized C* emission to the intrinsic C* emission in the absence of CCP. Efficient FRET from CCP to C* is a prerequisite for high signal amplification. Eq. (1) describes the calculation of FRET rate (K_{FRET}) (Förster, 1948):

$$K_{FRET}(r_{DA}) \propto \frac{1}{\tau_D}\left(\frac{R_0}{r_{DA}}\right)^6 \quad (1)$$

$$R_0 = \left[\frac{9000(\ln 10)Q_D\kappa^2 J(\lambda)}{128\pi^5 N n^4}\right]^6, \quad J(\lambda) = \frac{\int_0^\infty F_D(\lambda)\varepsilon_A(\lambda)\lambda^4\,d\lambda}{\int_0^\infty F_D(\lambda)\,d\lambda}$$

where r_{DA} is the donor/acceptor distance, τ_D is the lifetime of donor in the absence of acceptor, and R_0 is known as the Förster distance. Q_D is the quantum yield of the donor in the absence of acceptor, N is Avogadro's number, n is the refractive index of the medium, and k is the orientation factor. The overlap integral, $J(\lambda)$, expresses the degree of spectral overlap between the donor emission, $F_D(\lambda)$, and the absorption of acceptor, $\varepsilon_A(\lambda)$. The Förster equation is valid for ideal FRET processes where the donor and acceptor have well matched energy levels (Halls et al., 1999). When the energy levels of the acceptor are not contained within the orbital energies of the donor, photoinduced charge transfer (PCT), a competing process to FRET, is likely to occur. This could result in low acceptor emission and a deviation from the Förster equation (Brédas et al., 2004).

Electrostatic attractions between positively charged CCP and negatively charged phosphate groups in DNA-C* play an important role in bringing CCP and DNA-C* into close proximity to meet the FRET distance requirement (Gaylord et al., 2002; Xu et al., 2004). Different from ideal FRET systems where the distance between the donor and the acceptor is fixed, the distance between CCP and C* varies due to the dynamic complex structures of CCP/DNA-C*. Within CCP/DNA-C* complexes, there are cross-interaction between CCP and C* and self-interaction among C* or CCPs (Liu and Bazan, 2006b). Close association between CCP and DNA-C* favors FRET; whereas, self-interaction among CCPs leads to polymer aggregation, which reduces the polymer quantum yield in solution. Self-interaction among C* causes dye fluorescence quenching, ultimately leading to reduced signal amplification. To achieve high C* emission, it is thus necessary to optimize the FRET conditions, such as to increase the donor quantum yield, to improve the spectral overlap and orientation and to shorten the distance between donor/acceptor pairs. In addition, it is also important to select donor/acceptor pairs with well-matched energy levels and to develop strategies that could solve the fluorescence quenching of CCP or C* upon CCP/DNA-C* complex formation.

To improve the detection sensitivity of CCP-based DNA sensors, initial efforts were made towards optimization of various parameters shown in the Förster equation, which are summarized in our previous review (Liu and Bazan, 2004a). We have shown that both the polymer backbone structure and the side chain length affect the FRET efficiency (Liu et al., 2003a,b). Improved signal amplification has been demonstrated with shape-adaptable CCP where increased conformational freedom and improved registry with the analyte shape favors more efficient FRET relative to its linear counterparts (Liu et al., 2003b). Improved spectral overlap between a dual color polymer and a fluorescent dye is also reported to show improved signal amplification (Liu and Bazan, 2004b).

In this contribution, we review our recent efforts (after the previous review) in optimizing the CCP-sensitized signaling C* emission. Based on the understanding of donor/acceptor interactions within CCP/ssDNA-C* complexes, we developed different strategies from both materials and assay points of view in order to achieve a high signal output of C* emission. The strategies used for the materials include (1) optimizing molecular orbital energy

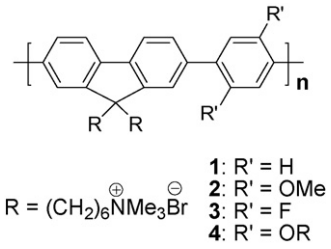

Scheme 1. Chemical structures of the CCPs, **1**–**4**.

levels (Liu and Bazan, 2006b), (2) reducing charge density (Pu et al., 2008a), (3) varying molecular architectures (Liu et al., 2007), and (4) adopting oligomeric approach (Liu and Dishari, 2008). The strategies used for the modification of assays include introducing (1) co-solvent (Liu and Bazan, 2007), (2) acceptor dilution (Liu and Bazan, 2006b), (3) surfactant (Pu et al., 2008b), and (4) nanoparticle (Wang and Liu, 2007).

1.1. Donor chemical structures

As energy donors, the physical properties of CCPs have a high impact on FRET efficiency (Liu and Bazan, 2004a). Development of different CCPs for high signal amplification of CCP-based DNA biosensors is of particular interest. For all CCPs involved in this review, a two-step synthetic strategy is used, which involves the synthesis of a neutral polymer, followed by post-polymerization (Liu and Bazan, 2004a, 2005, 2006a, 2007). The neutral conjugated polymers are obtained from the Suzuki polymerization of a dioxaborolane-substituted monomer and a dibromo-substituted monomer. Treatment of the neutral polymers with trimethylamine in THF/water gives the CCPs.

1.1.1. Molecular orbital energy levels

In view of inherent optoelectronic properties of CCP, PCT is one of the most detrimental processes for FRET (Brédas et al., 2004). The competition between FRET and PCT is determined by the energy level alignment between CCP and C*. A series of cationic poly(fluorene-*co*-phenylene) (PFP) derivatives (**1**, **2**, **3** and **4**, chemical structures shown in Scheme 1) was synthesized to investigate the effect of donor/acceptor energy levels on energy transfer(Liu and Bazan, 2006b). Fluorescein-(Fl) or Texas Red-(TR) labeled ssDNA$_1$ (sequence: 5′-ATC TTG ACT ATG TGG GTG CT-3′) were chosen as the energy acceptor. The emission spectra of **1**, **2**, **3** and **4** are similar, which have emission maxima at 415, 410, 414 and 410 nm, respectively. The normalized emission spectrum of PFP (**1**), and the absorption spectra of F1 and TR are shown in Fig. 1. The overlap between the emission of **1**–**4** and the absorption of F1 or TR is thus similar. The electrochemical properties of **1**–**4** were determined by cyclic voltammetry experiments. The calculated HOMO and LUMO levels are (−5.6 and −2.8 eV) for **1**, (−5.4 and 2.6 eV) for **2**, (−5.8 and −2.7 eV) for **3**, and (−5.4 and −2.6 eV) for **4**, respectively. Fluorine substitution lowers the energy levels by ∼0.2 eV, while the methoxy groups raise the levels by ∼0.2 eV, relative to those of **1**. The LUMO energy of Fl (−3.6 eV) is contained within the band gap of polymers **1**–**4**. However, the HOMO energy of Fl (−5.9 eV) is lower than that of **1** (−5.6 eV), **2** (−5.4 eV) and **4** (−5.4 eV). As a consequence, PCT process could occur between **1**, **2** or **4**, and Fl, and to less extend between **3** and Fl. The HOMO energy of TR (−5.4 eV) is higher than that of **1** and **3** and is close to that of **2**. From the HOMO–LUMO energy level point of view, TR matches **1**–**4** better than F1.

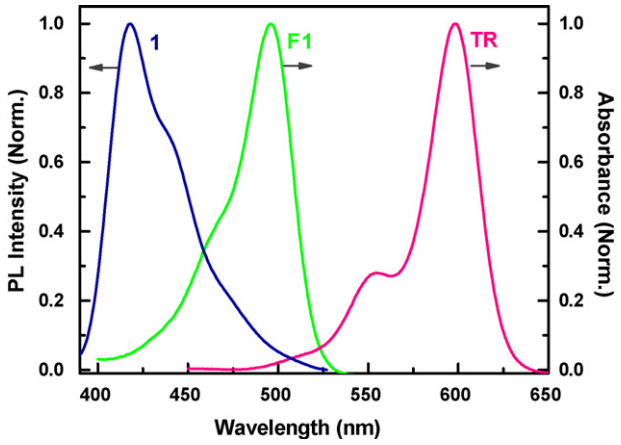

Fig. 1. The normalized emission spectrum of **1**, and the absorption spectra of F1 and TR.

FRET experiments between **1**–**3** and ssDNA$_1$-F1 or ssDNA$_1$-TR were performed by monitoring dye emission upon excitation of **1** (385 nm), **2** (365 nm), and **3** (365 nm). The results are shown in Fig. S1 (in the Supporting Information). The polymer concentrations were based on polymer repeat unit (RU). The most intense Fl emission was observed for **3**/ssDNA$_1$-Fl, which is approximately twofold more intense than that for **1**/ssDNA$_1$-Fl and is over an order of magnitude higher than that for **2**/ssDNA$_1$-Fl. For **3**/ssDNA$_1$-Fl, the integrated Fl emission is approximately fivefold greater than that obtained by direct excitation of Fl at its absorption maximum (495 nm) in the absence of **3**. In contrast to the low F1 emission for **2**/ssDNA$_1$-F1, TR emission from **2**/ssDNA$_1$-TR is much higher (Fig. S1b). This is due to better-matched energy levels between **2** and TR than that for 2/F1. This study indicates the importance of energy level alignment between the donor and acceptor in determining the CCP-sensitized dye emission.

1.1.2. Charge density

Apart from the electronic properties of CCP, the charge-mediated complexation between CCP and DNA-C* was also found to affect the polymer sensitized dye emission (Liu and Bazan, 2004a, 2006a). In this respect, the effect of charge density on CCP-sensitized C* emission was investigated using three cationic polyfluorene (PF) derivatives (**5**, **6** and **7** shown in Scheme 2) (Pu et al., 2008a,b). The facile functionality at fluorene C-9 position provides an opportunity to vary the side chains of cationic PFs without substantially changing their optoelectronic properties. Based on the previous study (Liu and Bazan, 2006b), ssDNA$_1$-TR was chosen as

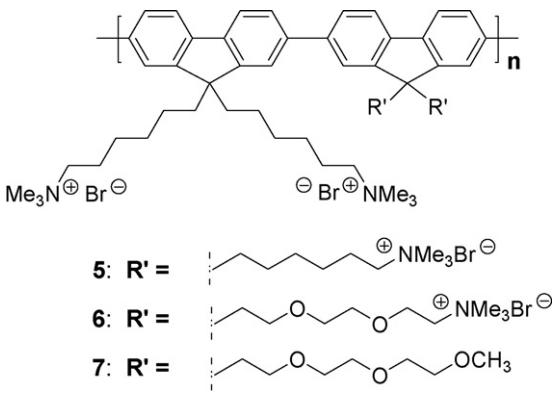

Scheme 2. Chemical structures of the CCPs, **5**–**7**.

the signaling probe to minimize the interference of PCT process and to facilitate the study of charge density effect.

The absorption and emission spectra of **5**, **6** and **7** in water are similar due to the same electronic backbone structure. The emission maxima for **5**, **6**, and **7** are 426, 421 and 426 nm, respectively. Similar overlap between the polymer emission and TR absorption is present. Polymers **5**, **6**, and **7** have similar quantum yields in water, which were measured to be 0.46, 0.50, and 0.50, respectively. Energy transfer studies between **5**–**7** and $ssDNA_1$-TR were conducted in water at fixed [$ssDNA_1$-TR] = 2×10^{-8} M (based on strands) with φ (φ is the ratio of polymer positive charges relative to ssDNA negative charges) ranging from 0 to 1.05. The largest difference in TR emission intensity for **5**/$ssDNA_1$-TR relative to **6**/$ssDNA_1$-TR and **7**/$ssDNA_1$-TR is observed at $\varphi = 1.05$ where [RU] = 2.1×10^{-7} M. The corresponding emission spectra of CCP/$ssDNA_1$-TR upon excitation of CCP at 385 nm at $\varphi = 1.05$ are shown in Fig. S2 (in the Supporting Information). It can be seen that the sensitized TR emission from **7**/$ssDNA_1$-TR is 2.3-fold more intense than that for **5**/$ssDNA_1$-TR, and is 3.6-fold more intense than that for **6**/$ssDNA_1$-TR. Detailed study of the TR fluorescence quenching upon $ssDNA_1$-TR/CCP complex formation reveals that the fluorescence quenching of TR emission is the lowest for $ssDNA_1$-TR/**7**. The origin of reduced TR fluorescence quenching is due to the increased TR–TR distance within the **7**/ssDNA-TR complexes. These data highlight that reduction of the CCP charge density can lead to increased CCP-sensitized C* emission mainly as a result of the reduced C* fluorescence quenching within the CCP/DNA-C* complexes.

1.1.3. Architecture effect

According to the Förster equation, a large orientation factor (k) is beneficial for high FRET efficiency. A water-soluble cationic tetrahedral molecule **9** was synthesized together with its arm molecule **8** (Scheme 3) (Liu et al., 2007). Molecules **8** and **9** have emission maxima at 400 and 408 nm, respectively. Good overlap between the emission of **8** and **9** with the absorption of F1 is observed. FRET measurements were carried out at fixed [dsDNA-Fl] = 2×10^{-8} M (dsDNA-Fl was obtained by hybridization of the $ssDNA_1$-Fl with $ssDNA_2$: 5′-AGC ACC CAC ATA GTC AAG AT-3′), with the fluorene unit (FU) concentration varying from 0 to 1.2×10^{-6} M. Fig. S3 (in the supporting information) compares the Fl emission from **1**/dsDNA-Fl and **8**/dsDNA-Fl, **9**/dsDNA-Fl upon excitation **1** and **9** at 358 nm, and **8** at 343 nm. Under the same [FU], **9** provides the highest Fl emission intensity. The amplification factor of F1 by **9** is 5.5, which is 2.2-fold larger than that by **1** (2.5). This improvement should arise from the fact that **9** provides for multiple-transition dipole moment orientations relative to the linear counterpart polymer **1**.

Fig.S4 (in the Supporting Information) shows the comparison of FRET between **1** and **9** to dsDNA-F1 and $ssDNA_1$-F1 at [$ssDNA_1$-Fl or dsDNA-Fl] = 2.0×10^{-8} M at [FU] = 1.2×10^{-6} M. The integrated Fl emission from **9**/dsDNA-Fl is over twofold more intense than that from **9**/$ssDNA_1$-Fl, and there is no significant difference observed between **1**/$ssDNA_1$-F1 and **1**/dsDNA-F1. These results indicate that **9** has shown improved selectivity between dsDNA and ssDNA as compared to **1**.

1.1.4. Oligomeric approach

Molecules **10**–**13** (Scheme 4) were designed to understand how the donor sensitized ssDNA-C* emission varying with the number of monomer repeat units (Liu and Dishari, 2008). The emission maxima for **10**, **11**, **12**, and **13** are 392, 404, 410, and 412 nm, respectively. FRET experiments were conducted using **10-13** as the donor and dsDNA-Fl as the acceptor. The results were compared with the counterpart polymer **5**. There was an increase in Fl emission upon addition of all the donors to dsDNA-Fl ([$dsDNA_1$-Fl] = 1×10^{-8} M) when [FU] was in the range of 0 to 4×10^{-7} M. Within the tested donor concentration range, the most intense donor sensitized Fl emission was observed for **13**, and the lowest was observed for **5**. The intensity of donor-sensitized Fl signal follows the following trend: **13** > **12** > **11** ≈ **10** > **5**.

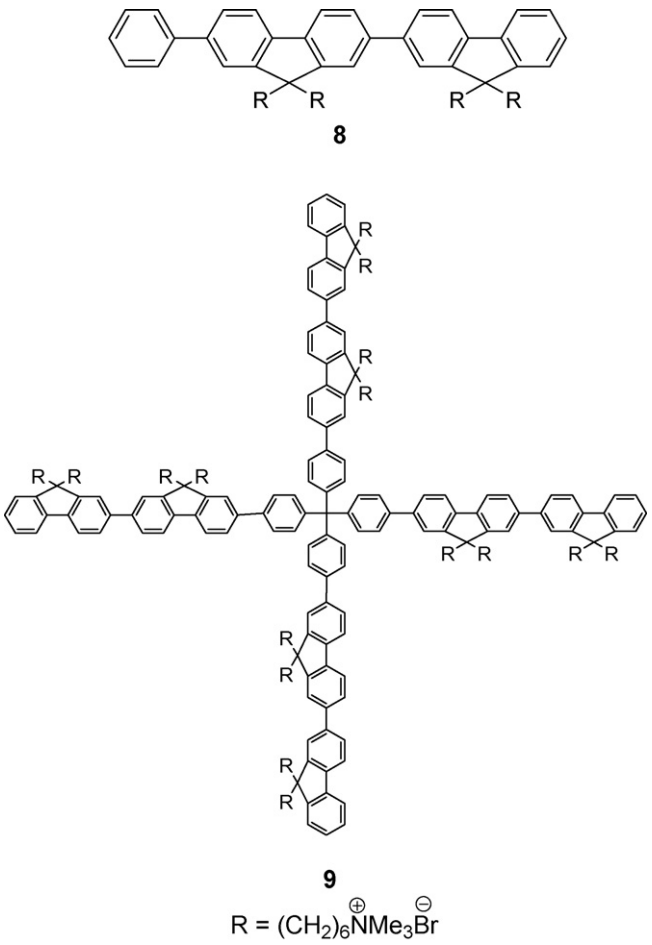

Scheme 3. Chemical structures of **8** and **9**.

Based on more efficient energy transfer between **13** and dsDNA-Fl, **13** was used as a representative oligomer in an energy transfer assay for DNA hybridization detection. A comparison of the solution spectra for energy transfer from **13** and **5** to dsDNA-Fl and $ssDNA_1$-Fl is shown in Fig. S5 (in the Supporting Information). In this figure, the emission spectra are normalized with respect to the residual emission of each donor. At [dsDNA-Fl or $ssDNA_1$-Fl] = 1.0×10^{-8} M and [FU] = 3×10^{-7} M, more intense donor sensitized Fl emission was observed for **13** to both dsDNA-Fl and $ssDNA_1$-Fl, as compared to that for **5**. The Fl emission intensity from **13**/dsDNA-Fl was over twice more intense than that from **13**/$ssDNA_1$-Fl. Under similar conditions, much less difference in Fl emission intensity was observed

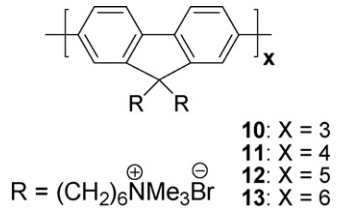

Scheme 4. Chemical structures of the oligomers **10**–**13**.

for **5**/dsDNA-Fl and **5**/ssDNA$_1$-Fl upon excitation of **5** at 411 nm. This study indicates that well-defined oligomers could serve as more efficient energy donors to enhance both sensitivity and selectivity of polymer-based fluorescent DNA assays.

1.2. Optimization of conditions for assay operation

Although modification of the donor molecules improves the signal amplification, materials synthesis is always time-consuming, laborious and at high cost. In addition, it is difficult to incorporate all the desired properties within a single donor molecule. As a consequence, some of our efforts were made to optimize the assay operation conditions. Co-solvent (Liu and Bazan, 2007), acceptor dilution (Liu and Bazan, 2006b), surfactant (Pu et al., 2008a,b) and nanoparticles (Wang and Liu, 2007) were used to modify the internal interactions within CCP/DNA-C* complexes, relied on which different extent of improvement in donor sensitized signal dye emission has been accomplished.

1.2.1. Co-solvent

Both CCP and DNA-C* are amphiphilic molecules (Pinto and Schanze, 2002; Liu and Bazan, 2004a). The hydrophobic interactions also participate in the CCP/DNA-C* complexation in conjugation with electrostatic attractions (Liu et al., 2003a). Thereby, introduction of water–miscible organic solvents into CCP-based DNA assay affects the donor/acceptor interactions within the CCP/DNA-C* complexes. The organic solvent/buffer mixture also disfavors PCT due to the decreased dielectric constant of the solvent mixture as compared to that for buffer (Brédas et al., 2004). On the basis of these considerations, **4** and ssDNA$_1$-F1 are chosen as the donor and accepter, respectively, and THF is chosen as the co-solvent (Liu and Bazan, 2007). Since the HOMO (−5.4 eV) and LUMO (−2.6 eV) energy levels of **4** are higher than those of Fl (−5.9 and −3.6 eV), change transfer between **4** and F1 is possible. The absorption and emission spectra of **4** in aqueous buffer (25 mM sodium phosphate, pH 7.4) and in a 50:50 (v/v) solution in THF/buffer are similar. The spectral overlap between the emission of **4** and the absorption of Fl in buffer is not significantly different from that in THF/buffer.

FRET from **4** to ssDNA$_1$-Fl was examined in buffer in the absence and presence of THF. Measurements were made at fixed [ssDNA$_1$-Fl] = 2×10^{-8} M and over a range of polymer concentrations ([RU] = 0–6×10^{-7} M). Fig. S6 (in the supporting information) shows the Fl emission from **4**/ssDNA$_1$-Fl in buffer and THF/buffer upon excitation of **4** ([RU] = 6×10^{-7} M) at 363 nm. Considerably more intense Fl emission was observed in the THF/buffer mixture as compared to that in buffer, which resulted from the reduced PCT and the weakened association between **4** and ssDNA$_1$-F1 in THF/buffer.

1.2.2. Dilution

Complexation between ssDNA-C* and CCP can lead to an increase in the local ssDNA-C* concentration relative to the same amount of ssDNA-C* in solution in the absence of CCP (Bazan, 2007; Liu and Bazan, 2004a). This causes C* fluorescence quenching, ultimately giving rise to weak signal output. To reduce C* fluorescence quenching within the complexes, dilution of ssDNA-C* with unlabeled ssDNA of an identical nucleotide sequence has been demonstrated to be effective (Liu and Bazan, 2006b).

For a typical dilution procedure [ssDNA$_1$] = 1.8×10^{-7} M was used to dilute the solution of [ssDNA$_1$-TR] = 2×10^{-8} M. TR emission was monitored upon direct excitation at 590 nm in the presence of different amount of **1**, **2**, and **3** (shown in Fig. S7 in the Supporting Information). F and F_0 represent the TR emission intensity in the presence and absence of CCP, respectively. There is virtually no quenching observed for TR upon interaction with **3** under these conditions, and there is only 15% loss of TR emission observed in the presence of **1**. Note that under similar conditions with [ssDNA$_1$-TR] = 2×10^{-8} M in the absence of ssDNA$_1$, addition of **1**, **2** and **3** to ssDNA$_1$-TR solution causes 70%, 80% and 60% decrease in TR intensity, respectively. Comparison between these two sets of data indicates that the TR fluorescence quenching upon complex formation is greatly reduced as a result of acceptor dilution.

FRET experiments were carried out under the optimum condition where the ratio of [DNA-TR] to [DNA] = 1:9. In the presence of [**3**] = 4×10^{-6} M [ssDNA$_1$-TR] = 2×10^{-8} M and [ssDNA$_1$] = 1.8×10^{-7} M, the polymer sensitized TR emission is 18-fold more intense than the intrinsic TR emission upon direct excitation of TR in the absence of the polymer. Under the same conditions, an amplification factor of 2 was obtained without acceptor dilution. The net effect of dilution is thus a 9-fold increase in CCP-sensitized TR emission intensity (upon excitation of **3**).

1.2.3. Surfactant

On the basis of our previous report that C* quenching within CCP/DNA-C* complexes is less severe in the presence of low charge density polymers as compared to that with high charge density polymers (Pu et al., 2008a), a new strategy is developed by using surfactant to partially neutralize the charges of CCP (Pu et al., 2008b). An anionic surfactant (sodium dodecyl sulphate, SDS) was used to regulate the microenvironment of CCP and DNA-C*. FRET experiments between **1** and ssDNA$_1$-TR in the absence and presence of SDS were conducted. The presence of SDS in solution affects both the optical properties of **1** and TR within **1**/ssDNA$_1$-TR complexes. The quantum yield of **1** decreases in the presence of SDS ([SDS] < 8.1 mM, CMC), which is detrimental for FRET. On the other hand, SDS reduces TR fluorescence quenching, which is beneficial for CCP-sensitized acceptor emission. This conflicting effect of SDS on the FRET process improves signal output to an extent which is dependent on SDS concentration. For [ssDNA$_1$-TR] = 2×10^{-8} M, an amplification factor of 12 and 1.5 was obtained for TR in the presence of 5 μM SDS and in the absence of SDS, respectively. The surfactant-enhanced CCP-sensitized dye emission reflects the importance of reducing the accepter fluorescence quenching in improving signal amplification.

1.2.4. Nanoparticle-assisted assays

Although the dye fluorescence quenching within CCP/DNA-C* complexes could be adjusted through the introduction of co-solvent, surfactant or acceptor dilution, to further reduce the acceptor fluorescence quenching, we developed a nanoparticle (NP)-based DNA assay (Scheme 5) (Wang and Liu, 2007). Polymer **3** and ssDNA$_1$-F1 were chosen as the donor molecule and the signaling probe, respectively, based on their optimum energy level alignment for FRET (Liu and Bazan, 2006b). The probe (5′-NH$_2$-ssDNA$_2$) was first immobilized onto silica nanoparticles (~400 probes/NP), which was followed by hybridization with ssDNA$_1$-F1 of varying concentrations. There was a linear increase in the total number of ssDNA$_1$-F1 molecules captured by each NP when [ssDNA$_1$-F1] was in a range of 0 to 3 μM, which was followed by saturation at higher [ssDNA$_1$-F1]. From the fluorescence change of ssDNA$_1$-F1 solutions before and after hybridization and removal of NPs, the number of ssDNA$_1$-F1 strands captured by each NP was calculated to be on the average $\sim 7 \pm 1$ for 0.18 μM, $\sim 24 \pm 2$ for 0.75 μM, and $\sim 56 \pm 5$ for 2.0 μM, respectively.

Upon excitation at 490 nm, the solution fluorescence increases almost linearly from 7ssDNA$_1$-F1/NP to 56ssDNA$_1$-F1/NP, indicating that there is almost no Fl fluorescence quenching on the NP surface. At a charge ratio (CCP/DNA probe and ssDNA$_1$-F1, +/−) of 3.2, upon excitation of **3** at 370 nm, the Fl emission intensity is the

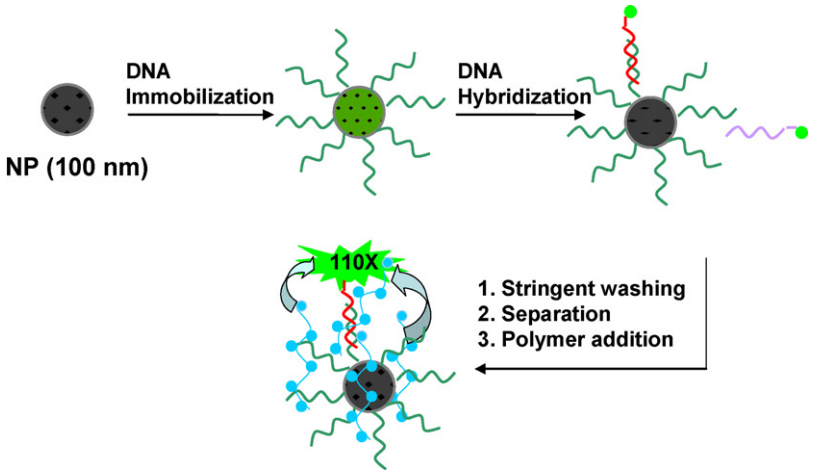

Scheme 5. Scheme of a NP-assisted CCP-based DNA assay.

highest for CCP/56ssDNA$_1$-F1/NP, which is approximately 40% more intense as compared to that for CCP/24ssDNA$_1$-F1/NP and is about 4-fold greater than that for CCP/7DNA$_1$/NP. However, the amplification factor increases from 40 for CCP/56ssDNA$_1$-F1/NP to 110 for CCP/7ssDNA$_1$-F1/NP. The F1 emission spectrum of **3**/7DNA$_1$-Fl/NP upon excitation of **3** at 370 nm is shown in Fig. S8 (in the Supporting Information). Direct excitation of the same amount of Fl at 490 nm in the absence of **3** is also shown for comparison. Under similar experimental conditions, a solution of free ssDNA$_1$-F1 with [Fl] the same as that of 7ssDNA$_1$-F1/NP generated only 14-fold signal amplification. Monitoring Fl emission upon direct excitation in the absence and presence of CCP showed no obvious intensity change observed for ssDNA$_1$-F1/NP solutions, which indicated that Fl quenching upon ssDNA$_1$/CCP complex formation is minimized with NP-based sensor design. The NP based assay also provides the advantage to increase the local concentration of donor units due to complexation between CCP and unhybridized probes on the NP surface. This assay allows detection of target DNA with a limit concentration of 10 pM, using a standard fluorometer.

2. Summary and conclusions

Our recent publications summarized in this review elucidate that CCP/DNA-C* complexation strongly determines intermolecular distances and FRET efficiencies. To optimize the energy transfer between CCPs and C*-labeled DNA, one first needs to consider the donor/acceptor energy levels and the fluorescence behavior of the donor or the acceptor within the CCP/DNA-C* complexes in addition to spectral overlap, orientation and distance between the donor and the acceptor. Mismatched energy levels can lead to PCT, which competes with the FRET process. This problem could be solved by the introduction of functional groups on the polymer backbone to fine-tune the HOMO and LUMO energy levels of the donor. With the same electronic backbone structure, further improvement in energy transfer can be accomplished by reducing the charge density of CCPs. Comparison of the optical properties and sensing behaviors between the oligomers and the corresponding polymer revealed the advantage of oligomeric molecules over polymers for biosensor applications. Moreover, oligomeric tetrahedral molecules provide increased conformational freedom and improved registry with the analyte shape, which favors more efficient FRET relative to its linear counterparts. On the other hand, small variations in the assay operation conditions, such as the introduction of co-solvent, surfactant or dilution of the acceptor, could also modify the interactions between CCP and DNA-C* within the complexes, which yield high polymer sensitized dye emission. Combination of the best polymer **3** with a nanoparticle-assisted assay leads to a signal amplification factor of over 110. This strategy not only takes advantage of the minimized C* fluorescence quenching, but also allows excess DNA probes on the NP surface to capture CCPs to increase the local concentration of donor units and deliver excitations to C*. Relied on the NP-assisted assay, the detection limit for DNA is 10 pM, using a standard fluorometer. On the other hand, with poly(thiophene) amplified dye signal, zeptomole sensitivity has been reported by Leclerc et al. using a custom-made detection instrument (Ho et al., 2005). Since the physiologically significant level of DNA concentration is reported to be in the femtomolar range (Ye and Ju, 2003), we thus believe that conjugated polymer amplified assays could be used directly for physiological samples. As compared to other methods that have been used to improve fluorescent assay sensitivity, such as using multiple-labeled probes (Yang et al., 2005), dye-doped silica nanoparticle-based probes (Zhao et al., 2003), or surface plasmon (Sabanayagam and Lakowicz, 2007), use of conjugated polymers does not require complicated labeling of probes or specific instruments and should be applicable to many standard fluorescent assays.

3. Future perspectives

From a practical perspective, the conjugated molecule behaves as a light-harvesting antenna that can be used to amplify the emission intensities of diagnostic chromophores, which has superior sensitivity as compared to single fluorophore assays. Fine-tuning of donor/acceptor optical properties and optimization of assay operation conditions should lead to biosensors for real time applications. Clear challenges include the syntheses of water-soluble conjugated polymers with a large range of emission frequencies, high fluorescence quantum yields, different charges, and specific molecular architecture that more clearly differentiate the secondary and tertiary structures of biomolecules. Designing new optical platforms will require perfect balancing of the properties of donor and acceptor, and thorough understanding of the interactions within the donor/acceptor complexes. Further improvement in overall signal amplification and sensitivity of CCP based optical sensors could be realized with a methodology involving the concurrent virtues of enhancing the quantum yield of CCP and reducing the acceptor quenching within the complexes. Although conjugated polymers have been used with bioprobes for DNA detection, and the assays have shown advantages of easy operation and quick response with

moderate to high sensitivity, the interference of the polymer emission tail at the long wavelength with the dye emission needs to be addressed.

Acknowledgements

The authors are grateful to the National University of Singapore (ARF R-279-000-197-112/133, R-279-000-233-123 and YIA R-279-000-234-123), and Singapore Ministry of Education (R-279-000-255-112) for financial support.

Appendix A. Supplementary data

Supplementary data associated with this article can be found, in the online version, at doi:10.1016/j.bios.2008.07.029.

References

Avouris, P., Chen, J., 2006. Mater. Today 9, 46–54.
Bäuerle, P., Emge, A., 1998. Adv. Mater. 10, 324–330.
Bazan, G.C., 2007. J. Org. Chem. 72, 8615–8635.
Boon, E.M., Ceres, D.M., Drummond, T.G., Hill, M.G., Barton, J.K., 2000. Nat. Biotechnol. 18, 1096–1100.
Brédas, J.L., Beljonne, D., Coropceanu, V., Cornil, J., 2004. Chem. Rev. 104, 4971–5004.
Bruchez, M., Moronne, M., Gin, P., Weiss, S., Alivisatos, A.P., 1998. Science 281, 2013–2016.
Cardullo, R.A., Agrawal, S., Flores, C., Zamechnik, P.C., Wolf, D.E., 1988. Proc. Natl. Acad. Sci. U.S.A. 85, 8790–8794.
Chan, W.C.W., Nie, S.M., 1998. Science 281, 2016–2018.
Chen, L., McBranch, D.W., Wang, H., Helgeson, R., Wudl, F., Whitten, D., 1999. Proc. Natl. Acad. Sci. U.S.A. 96, 12287–12292.
Dubertret, B., Calame, M., Libchaber, A., 2001. Nat. Biotechnol. 19, 365–370.
Ewbank, P.C., Nuding, G., Suenaga, H., McCullough, R.D., Shinkai, S., 2001. Tetrahedron Lett. 42, 155–157.
Fan, C., Plaxco, K.W., Heeger, A.J., 2003. Proc. Natl. Acad. Sci. U.S.A. 100, 9134–9137.
Förster, T., 1948. Ann. Phys. 2, 55–75.
Gaylord, B.S., Heeger, A.J., Bazan, G.C., 2002. Proc. Natl. Acad. Sci. U.S.A. 99, 10954–10957.
Gaylord, B.S., Heeger, A.J., Bazan, G.C., 2003. J. Am. Chem. Soc. 125, 896–900.
Halls, J.J.M., Comil, J., Santos, D.A., Silbey, R., Hwang, D.H., Holmes, A.B., Brédas, J.L., Friend, R.H., 1999. Phy. Rev. B 60, 5721–5727.
Herland, A., Inganäs, O., 2007. Macromol. Rapid Commun. 28, 1703–1713.
Ho, H., Leclerc, M., 2004. J. Am. Chem. Soc. 126, 1384–1387.
Ho, H., Doré, K., Boissinot, M., Bergeron, M.G., Tanguay, R.M., Boudreau, D., Leclerc, M., 2005. J. Am. Chem. Soc. 127, 12673–12676.
Kim, I.B., Erdogan, B., Wilson, J.N., Bunz, U.H.F., 2004. Chem. Eur. J. 10, 6247–6254.
Korri, Y.H., Garnier, F., Srivastava, P., Godillot, P., Yassar, A., 1997. J. Am. Chem. Soc. 119, 7388–7389.
Leclerc, M., 1999. Adv. Mater. 11, 1491–1498.
Lee, D.W., Swager, T.M., 2004. Synlett, 149–154.
Liu, B., Bazan, G.C., 2004a. Chem. Mater. 16, 4467–4476.
Liu, B., Bazan, G.C., 2004b. J. Am. Chem. Soc. 126, 1942–1943.
Liu, B., Bazan, G.C., 2005. Proc. Natl. Acad. Sci. U.S.A. 102, 589–593.
Liu, B., Bazan, G.C., 2006a. Nat. Protoc. 1, 1698–1702.
Liu, B., Bazan, G.C., 2006b. J. Am. Chem. Soc. 128, 1188.
Liu, B., Bazan, G.C., 2007. Chem. Asian J. 2, 499–504.
Liu, B., Dishari, S.K., 2008. Chem. Eur. J. 14, 7366–7375.
Liu, B., Gaylord, B.S., Wang, S., Bazan, G.C., 2003a. J. Am. Chem. Soc. 125, 6705–6714.
Liu, B., Wang, S., Bazan, G.C., Mikhailovsky, A., 2003b. J. Am. Soc. Chem. 125, 13306–13307.
Liu, B., Dan, T.T.T., Bazan, G.C., 2007. Adv. Funct. Mater. 17, 2432–2438.
Mannelli, I., Minunni, M., Tombelli, S., Mascini, M., 2003. Biosens. Bioelectron. 18, 129–140.
McQuade, D.T., Pullen, A.E., Swager, T.M., 2000. Chem. Rev. 100, 2537–2574.
Nam, J.M., Thaxton, C.S., Mirkin, C.A., 2003. Science 301, 1884–1886.
Nguyen, T.Q., Wu, J.J., Doan, V., Schwartz, B.J., Tolbert, S.H., 2000. Science 288, 652–656.
Nilsson, K.P.R., Inganäs, O., 2003. Nat. Mater. 2, 419–424.
Nuovo, G.J., 2000. Methods Mol. Biol. 123, 217–238.
Patolsky, F., Lichtenstein, A., Willner, I., 2001. Nat. Biotechnol. 19, 253–258.
Pinto, M.R., Schanze, K.S., 2002. Synthesis, 1293–1309.
Pinto, M.R., Schanze, K.S., 2004. Proc. Natl. Acad. Sci. U.S.A. 101, 7505–7510.
Pu, K.Y., Fang, Z., Liu, B., 2008a. Adv. Funct. Mater. 18, 1321–1328.
Pu, K.Y., Pan, Y.H., Liu, B., 2008b. J. Phys. Chem. B. 112, 9295–9300.
Sabanayagam, C.R., Lakowicz, J.R., 2007. Nucleic Acid Res. 35, e13.
Seferos, D.S., Giljohann, D.A., Hill, H.D., Prigodich, A.E., Mirkin, C.A., 2007. J. Am. Chem. Soc. 129, 15477–15479.
Sutherland, G., Mulley, J., 1989. In: Symons, R.H. (Ed.), In Nucleic Acid Probes. CRC Press, Florida, p. 159.
Swager, T.M., 1998. Acc. Chem. Res. 31, 201–207.
Thomas III, S.W., Joly, G.D., Swager, T.M., 2007. Chem. Rev. 107, 1339–1386.
Wang, J., 2000. Nucleic Acid Res. 28, 3011–3016.
Wang, Y., Liu, B., 2007. Chem. Commun., 3553–3555.
Xu, Q.H., Gaylord, B.S., Wang, S., Bazan, G.C., Moses, D., Heeger, A.J., 2004. Proc. Natl. Acad. Sci. U.S.A. 101, 11634–12221.
Yang, C.Y., Yang, H.L., Tan, W.H., 2005. J. Am. Chem. Soc. 127, 12772–12773.
Ye, Y.K., Ju, H.X., 2003. Sensors 3, 128–145.
Zhao, X.J., Tapec, D.R., Tan, W.H., 2003. J. Am. Chem. Soc. 125, 11474–11475.
Zhou, Q., Swager, T.M., 1995. J. Am. Chem. Soc. 117, 12593–12602.